Environ. Sci. Technol. **2010,** *44,* 3455–3461

Chemical Transformations during Aging of Zerovalent Iron Nanoparticles in the Presence of Common Groundwater Dissolved Constituents

BRIAN C. REINSCH,[†,‡] BRADY FORSBERG,[§] R. LEE PENN,[§] CHRISTOPHER S. KIM,[∥] AND GREGORY V. LOWRY*[,†,‡]

Department of Civil and Environmental Engineering, Carnegie Mellon University, Pittsburgh, Pennsylvania 152313, Center for the Environmental Implications of Nanotechnology (CEINT), Pittsburgh, Pennsylvania 15213, Department of Chemistry, University of Minnesota, Minneapolis, Minnesota 55455, and Department of Chemistry, Chapman University, Orange, California 92866

Received September 25, 2009. Revised manuscript received March 16, 2010. Accepted March 22, 2010.

Nanoscale zerovalent iron (NZVI) that was aged in simulated groundwater was evaluated for alterations in composition and speciation over 6 months to understand the possible transformations NZVI could undergo in natural waters. NZVI was exposed to 10 mN of various common groundwater anions (Cl^-, NO_3^-, SO_4^{2-}, HPO_4^{2-}, and HCO_3^-) or to dissolved oxygen (saturated, ~9 mg/L). Fresh and exposed NZVI samples, along with Fe-oxide model compounds, were then analyzed using synchrotron radiation X-ray absorption spectroscopy (XAS) to yield both relative oxidation state, using the X-ray absorption near edge structure (XANES), and quantitative speciation information regarding the types and proportions of mineral species present, from analysis of the extended X-ray absorption fine structure (EXAFS). Over 1 month of aging the dissolved anions inhibited the oxidation of the NZVI to varying degrees. Aging for 6 months, however, resulted in average oxidation states that were similar to each other regardless of the anion used, except for nitrate. Nitrate passivated the NZVI surface such that even after 6 months of aging the particles retained nearly the same mineral and Fe^0 content as fresh NZVI. Linear least-squares combination fitting (LCF) of the EXAFS spectra for 1 month-aged samples indicated that the oxidized particles remain predominantly a binary phase system containing Fe^0 and Fe_3O_4, while the 6 month aged samples contained additional mineral phases such as vivianite ($Fe_3(PO_4)_2 \cdot 8H_2O$) and iron sulfate species, possibly schwertmannite ($Fe^{3+}{}_{16}O_{16}(OH,SO_4)_{12-13} \cdot 10-12H_2O$). The presence of these additional mineral species was confirmed using synchrotron-based X-ray diffraction (XRD). NZVI exposed to water saturated with dissolved oxygen showed a rapid (<24 h) loss of Fe^0 and evolved both magnetite and maghemite (γ-Fe_2O_3) within the oxide layer. These findings have implications toward the eventual fate, transport, and toxicity of NZVI used for groundwater remediation.

Introduction

Nanoscale zerovalent iron (NZVI) is used for remediating groundwater contaminated with chlorinated solvents, heavy metals, and other reducible groundwater contaminants (*1*). NZVI surface modification by polymers and polyelectrolytes used to increase NZVI transport distances in the subsurface (*2*−*5*) to enable emplacement also increases the potential for unwanted exposures to sensitive biological receptors. NZVI will oxidize once deployed into the environment, either completely or partially from Fe^0 to various Fe oxides (*6*). The formation of other Fe-bearing mineral phases such as siderite and vivianite are also possible (*7, 8*). The rate and extent of oxidation and the types of mineral phases present on the NZVI surface will depend on the geochemical conditions under which the particles are exposed. The chemical composition and degree of oxidation of the nanoparticle will also affect magnetic moment and aggregation potential (*9*), reactivity (*10*), and toxicity (*11, 12*). Therefore, identifying the chemical alterations to the NZVI surfaces upon release to the environment is essential to understanding its immediate and long-term fate and toxicity (*11, 13*).

Nanoparticle aggregation depends on surface charge and, in the case of NZVI, the magnetic moment, which is highly dependent on the amount of Fe^0 (*9*). The surface charge of NZVI at environmental pH, and hence the behavior of NZVI in the environment and its associations with numerous aqueous and solid species, will depend on the types of Fe-mineral phases present on the particle surface because each species may have a different isoelectric point (IEP) value. Magnetite, maghemite, and goethite, for example, have IEP values of 6.0, 6.6, and 8.4 respectively (*14*), so particles may be positive or negatively charged at pH = 7 depending on the species present on the surface. Increased magnetic moment of NZVI has been shown to increase aggregation. Phenrat et al. showed that nonmagnetic nanoparticles, like hematite, aggregate less than magnetite and much less than NZVI (*9*). Thus, the Fe^0 content and the magnetic potential of oxide that forms will influence the stability against aggregation and mobility of NZVI, especially through porous media (*15*).

Previous studies have characterized NZVI in hopes of correlating the Fe-oxide phases present and their respective proportions to reactivity (*16, 17*). Aged/oxidized NZVI particles have lower redox activity and presumably lower reaction potential. The oxide layer of NZVI is considered to be passivating, and the overall activity of the particle may be dependent on the species at the surface. Magnetite, a conductive iron oxide (*14*), can provide a conductive medium between the reactive surface species in solution and the inner electron-rich core, whereas the presence of maghemite or hematite at the surface, both less conductive than magnetite, could potentially decrease the reactivity and rate of oxidation of zerovalent iron. It has been shown that an increased oxidation state of Fe in the particles decreases the cytotoxicity of NZVI to *E. coli* (*12*). The toxicity may also be affected by the species of oxide present at the surface, as goethite and hematite are ubiquitous, often are present as nanoparticles

* Corresponding author e-mail: glowry@andrew.cmu.edu; telephone: 412-268-2948; fax: 412-268-7813; address: Carnegie Mellon University, Department of Civil and Environmental Engineering, 5000 Forbes Ave., Pittsburgh, Pennsylvania 15213-3890.
[†] Carnegie Mellon University.
[‡] Center for the Environmental Implications of Nanotechnology.
[§] University of Minnesota.
[∥] Chapman University.

10.1021/es902924h
Published on Web 04/09/2010

in nature (*18*), and should be less detrimental to life than the more redox reactive NZVI (*12*).

Studies correlating NZVI properties to its reactivity, transport, and toxicity (*11, 12, 16, 19, 20*) have used a variety of destructive techniques that depend on chemical transformations (atomic emission spectroscopy (AES), atomic absorption (AA), gas chromatography (GC), inductively coupled plasma-mass spectrometry (ICP-MS)) for analysis or are limited in the ability to distinguish between structurally similar chemical Fe-mineral species such as magnetite and maghemite (X-ray diffraction, XRD) (*21*). Microscopy such as high resolution transmission electron microscopy (HRTEM) can be used to identify lattice fringe spacing of species but is limited to qualitative identification, do not provide concentration information, and is subject to human interpretation (*22*). As a result, for Fe systems that may contain oxides with similar structures (i.e., magnetite and maghemite), techniques that can effectively discriminate between such species are valuable.

Synchrotron-based X-ray absorption spectroscopy (XAS) is a technique that can provide the average oxidation state of a sample and quantitative identification of the proportion of Fe minerals within a system (*23*). X-ray absorption near edge structure (XANES) is sensitize to and is employed here as a means to measure the overall oxidation state of iron (*24, 25*). Extended X-ray absorption fine structure (EXAFS), the higher energy region of the XAS spectrum, is particularly sensitive to crystal structure (*24, 26*) and is used in this study to identify and quantify the mineral species within NZVI and those that are formed during exposure.

The potential mineralogical changes (i.e., weathering) NZVI particles may undergo when aged in the presence of groundwater constituents have not been reported. The objectives of this study were (1) to determine how common groundwater anions affect the rate and extent of oxidation over short and prolonged exposure, especially the previously noted (*27*) special ability of nitrate to passivate the NZVI surface toward reaction with trichloroethylene (TCE); (2) to determine the species of the oxide layer when aged in anaerobic water compared to the presence of dissolved oxygen; and (3) to determine if exposure to anions can lead to species other than the proposed Fe/magnetite core/shell structure. The systems described here represent a subset of reactions and transformations that NZVI may undergo when in contact with natural waters that often contain many more dissolved species than those included in this study.

Materials and Methods

Materials. Nitrate, sulfate, bicarbonate, phosphate, and chloride (all ≥99.0%) were all added, as their respective Na salts. Ultrahigh-purity Ar, N_2, and H_2 (5% balance N_2) were used in a glovebox atmosphere and were supplied by Butler Gas (Pittsburgh, PA). Reactive nanoscale iron particles (RNIP, synonymous with NZVI), were supplied by Toda Kogyo Corp. (Onoda, Japan) as an uncoated dried powder with the specific trade model name RNIP 10-DP and stored in an anaerobic glovebox prior to use. Nurmi et al. previously characterized RNIP 10-DS, a similar RNIP product that is provided as an aqueous slurry rather than a dry powder, and similar chemical and physical characteristics were found for our material, with the exception of what iron species exist within the oxide layer (*17*).

The model Fe-mineral species that comprised the model compound library were either purchased from commercial vendors or synthesized close to nanoscale as possible. Magnetite (≥99.5%) 15−20 nm, hematite (≥98%) 30−50 nm, and maghemite (≥96%) 20−50 nm were purchased from Nanostructured & Amorphous Materials Inc., Houston. The synthesis procedure for each model compound that was not purchased is included in the Supporting Information.

Batch Groundwater Anion Systems. NZVI particles (10 g/L) were aged for a period of 1 month and 6 months in 10 mN common groundwater anion solutions (NO_3^-, SO_4^{2-}, HCO_3^-, HPO_4^{2-}, and Cl^-) using unbuffered nanopure DI water that had been sparged with $N_{2(g)}$. Initial creation of the batch systems, aging, and pH measurements were conducted anaerobically, and the sealed reactors (60 mL Wheaton Serum bottles) were rotated end-over-end while aging at room temperature (22 °C). After 1 and 6 months, the sample bottles were opened and the pH was measured. The pH of the systems ranged from 8.7 to 10 after a month and had risen to 9.0−11.8 over 6 months. A series of reactors with varying concentrations of NO_3^- (0.2, 1, 3, 5, and 10 mN) was also prepared, aged for 1 month, and analyzed in the same fashion. This concentration range of nitrate was used because Liu et al. showed that reactors containing $[NO_3] > 3$ mN significantly decreased reactivity of NZVI with TCE. They reported an increase in inhibition between 3 and 5 mN but did not evaluate higher concentrations (*27*), so this study included a 10 mN concentration sample to see if a similar trend could be seen regarding passivation toward oxidation of the Fe^0 core. In all samples, the particles were isolated for analysis by holding them to the bottom of their reactors using a 200 lb pull-force magnet while the solution was decanted. The particles were dried completely using nitrogen gas flow and stored until analysis in a glovebox.

Oxidation in the Presence of Excess Dissolved Oxygen (DO). A 10 g/L batch of NZVI was allowed to age while ambient air was bubbled through in order to mimic an environmental system saturated with DO (∼9 mg/L). After 24 h, the particles were separated, dried, and stored anaerobically, as described above, until they were analyzed using synchrotron radiation as described below.

Model Compound Library. To successfully identify all mineral phases present in batch studies, a model compound database of nanosized Fe mineral extended X-ray absorption fine structure (EXAFS) spectra was compiled. The model compound library consisted of common Fe oxides, Fe hydroxides, and Fe-mineral phases that possibly could have formed from the reaction of groundwater anions (e.g., magnetite, maghemite, pyrite, schwertmannite, vivianite, goethite). A complete list of the model compounds along with their EXAFS spectra and other measured properties are provided in the Supporting Information (Figure S1). Samples of model compounds were dried anaerobically into powders and diluted into boron nitride powder prior to X-ray analysis. EXAFS spectra were collected using the same SSRL beamline and parameters described below and in the Supporting Information.

X-ray Absorption Spectroscopy (XAS) Analysis. Presented here is an abridged description of XAS data collection, data reduction, and analysis. A detailed description of the XAS method is included in the Supporting Information. XAS was conducted at Stanford Synchrotron Radiation Laboratory (SSRL) wiggler magnet beamline 10-2 under anaerobic conditions. Samples were stored, manipulated, transported, and analyzed under anaerobic conditions at all times. Fe K-edge (7112 eV) XAS spectra were collected at room temperature in transmission mode using a Fe calibration foil over the energy range 6879−7986 eV.

Data were analyzed using SixPACK software version 0.60 (*28*). XAS scans were calibrated to 7112.0 eV using the first derivative of the Fe calibration standard, averaged together, deglitched when needed, background subtracted with E_0 defined as 7125 eV, converted to frequency (k) space, and weighted by k^3. Principal component analyses (PCA) were also performed in SixPACK, which uses an algorithm described by Ressler et al. (*29*) and references therein, to determine the minimum number of components that could be used to model the sample set of 1 month and 6 month

aged NZVI EXAFS spectra, respectively, and account for >90% of the spectra. PCA was conducted in *k*-space in the *k*-range of 3 to 12 Å, 3 to 15 Å, 3 to 17 Å, depending on the quality of the data. In all cases, ≤3 components was a sufficient number to account for >90% of the spectra. The components determined from PCA were applied to least-squares combination fitting (LCF) to provide quantitative speciation information.

LCF of individual sample EXAFS spectra of model compounds were used to identify and quantify the mineral phases present in a sample, with the number of phases allowed to exist constrained to the number of components that was determined by PCA (≤3 components). LCF identified components should be considered accurate to ±25% of their stated values. Errors reported for individual components are calculated by SixPACK's least squared fitting module. Components representing less than 10% of a fit should be viewed with caution (*30, 31*). The linear least-squares fitting procedure employed was adapted from Kim et al. (*31*). The spectra were fit from a *k*-range of 3 to 12 Å, 3 to 15 Å, or 3 to 17 Å.

Synchrotron X-ray Diffraction (XRD) Analysis. Selected dried samples were analyzed at SSRL BL 11-3 using a MAR 345 flat plate detector at a sample to detector distance of 148.3 mm as determined through calibration with LaB_6. The beam measured 0.150 mm^2, and the energy of the beam was 12705 eV. This configuration resulted in a Q-range of 0−5.3 $Å^{-1}$. The image from the 150 $pixel^2$ detector was integrated in degrees 2θ using the Area Diffraction Program (*32*). Each diffraction pattern was background subtracted and peak matched using Xpert Highscore Plus, at the energy of the synchrotron beam, using peak positions and relative intensities as the identification parameters.

Results and Discussion

Effect of Groundwater Dissolved Solutes on NZVI Oxidation. Fresh NZVI particles have been reported by other investigators to consist of Fe^0 and Fe_3O_4 (*17, 20*). Oxidation of the particles should lead to an overall increased oxidation state of the particles from Fe^0 to Fe^{2+} to Fe^{3+} that is observable using XANES. The XANES regions of the XAS spectra for Fe K-edge XAS have distinctive separation of the adsorption edge for Fe^0, Fe^{2+}, and Fe^{3+}, with the more oxidized absorption edges occurring at higher energy (*24*). In this way, the relative extent of oxidation of a series of samples with systematic variance can be qualitatively compared (*25*). Figure 1 shows the Fe−K absorption edges for samples aged for 1 month. There is a 2 to 3 eV shift to higher energy of the XANES edge between the least and most oxidized samples. This type and magnitude of shift was noted by Waychunas et al. (*24*) for Fe minerals of varying oxidation states.

The samples aged over a period of 1 month show distinct degrees of passivation of the nanoparticle surface toward oxidation by water. The anions listed in increasing passivation ability are $HCO_3^- < HPO_4^{2-} < SO_4^{2-} < Cl^- < NO_3^-$. It has been noted previously that some anions in sufficiently high concentrations can passivate iron surfaces (*14, 27*) as determined from NZVI reactivity with TCE in water. Typically SO_4^{2-}, Cl^-, and HCO_3^- are considered major constituents of groundwater (10^{-3} to 10 mN), NO_3^- is a secondary constituent (10^{-4}−10^{-1} mN), and HPO_4^{2-} is usually a trace element (<10^{-5} mN) (*33, 34*). Therefore, exposures used here are at the high end of the expected range for SO_4^{2-}, Cl^-, and HCO_3^- and are higher than would be expected for NO_3^- and HPO_4^{2-}. After 6 months of aging, however, the degree of oxidation for most samples was similar to that of the sample aged in DI water, with nitrate being the notable exception. Nitrate passivated the surface sufficiently to prevent oxidation over 6 months (Figure 1B). Nitrate has been shown to passivate the surface of iron toward oxidation and reaction, and the mechanism of passivation has been proposed to be the formation of a protective oxide layer (*14*).

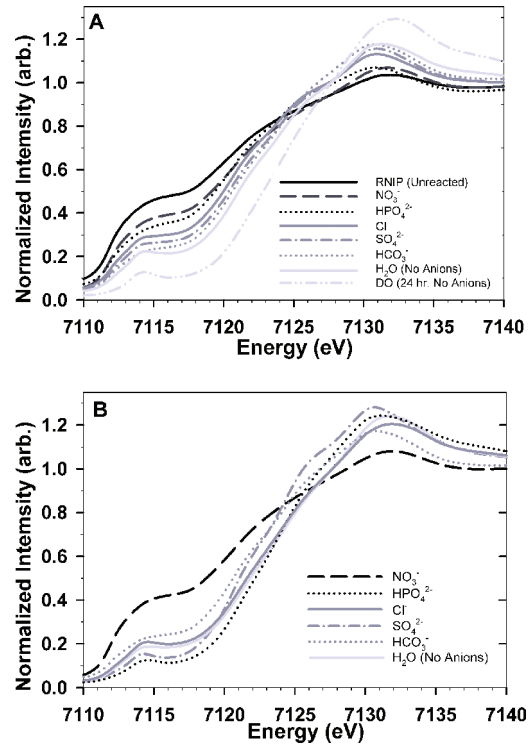

FIGURE 1. Relative oxidation state of NZVI aged anaerobically (except for DO) in the absence and presence of common groundwater anions (10 mN) after 1 month (A) and 6 months (B) represented as the Fe K-edge XANES. The legend is included within both graphs to aid in line identification. The relative positions of the curves represent the average oxidation state of the bulk sample with the most oxidized representing the largest absorption edge shift toward higher energy. (A) After only 1 month, there are varying degrees of passivation depending on anion, with just water and excess DO being the most oxidized. (B) The passivation effect has decreased; however, nitrate maintains a similar oxidation state.

Previous work by Liu et al. had suggested that the passivation of the NZVI surface by nitrate occurs at nitrate concentrations >3 mN (*27*). The reaction between NZVI and TCE was used to probe the particle reactivity, but no analysis of the NZVI was performed. Here, we look at the effects of nitrate on the surface properties of NZVI. XANES analysis of NZVI aged in different concentrations of nitrate showed that above 5 mN the centroid of the XANES absorption peaks are ~1 eV lower than those with <5 mN. Also, there was an exclusive bimodal distribution of oxidation states with respect to concentration (Figure 2). This suggests that NZVI oxidation is indeed limited in the presence of nitrate >5 mN. The mechanism for passivation at high nitrate concentration has been suggested to be the buildup of nitrite and subsequent formation of a passivating and insoluble Fe(III) oxide layer, like maghemite or hematite (*35*). However, neither maghemite, hematite, nor goethite was observed using EXAFS (discussed next), suggesting that the passivating layer is some other phase, is present at too low of a concentration to detect using EXAFS, or that saturation of reactive surface sites by nitrite may be enough to hinder oxidation by water (*36*).

NZVI Speciation and Additional Mineral Formation. The proposed model for the oxidation of NZVI is typically a progression from α-Fe^0 to Fe_3O_4, with a thickening of the oxide layer over time. Generally, this model has been backed by both TEM and XRD data (*17*). Other investigators have detected the presence of the more oxidized maghemite (γ-Fe_2O_3) in granular iron using micro-Raman spectroscopy (*37*).

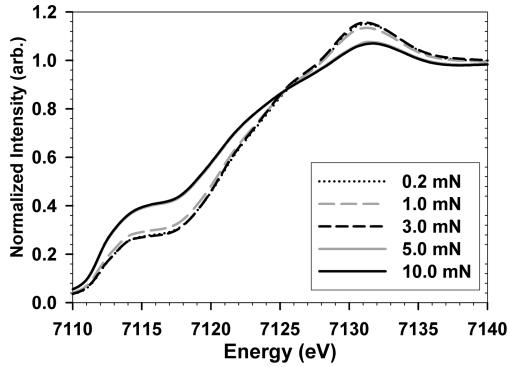

FIGURE 2. Passivation of nitrate as a function of concentration is shown in the Fe K-edge XANES of NZVI aged with varying concentrations of nitrate (0.2−10 mN) showing bimodal retardation of NZVI oxidation by water over 1 month. The higher concentrations retain an average particle oxidation state close to the original particle, with 5 mN and 10 mN sharing identical shape and position, whereas the lower concentrations of 0.2−3 mN advance to higher oxidation.

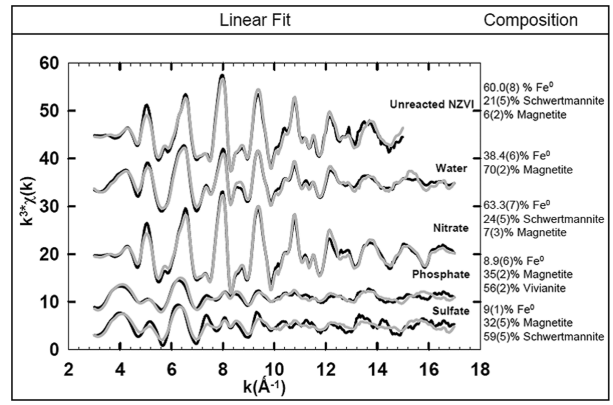

FIGURE 3. Transformation of NZVI over 6 months as shown by LCF of 6 month aged samples in 10 mN of the respective anions. Black = data, gray = fits. Quantitative results also listed to the right of the respective spectrum with uncertainty for the last digit in parentheses. From top to bottom: Unreacted NZVI is the dry starting material (RNIP 10-DP); particles aged in water are the control as no anions were present in solution and have shown significant oxidation; nitrate passivates the surface of NZVI so that the spectrum looks very similar to that of the unreacted material; phosphate promotes the formation of vivianite; and sulfate results in the formation of an iron sulfate mineral (possibly schwertmannite).

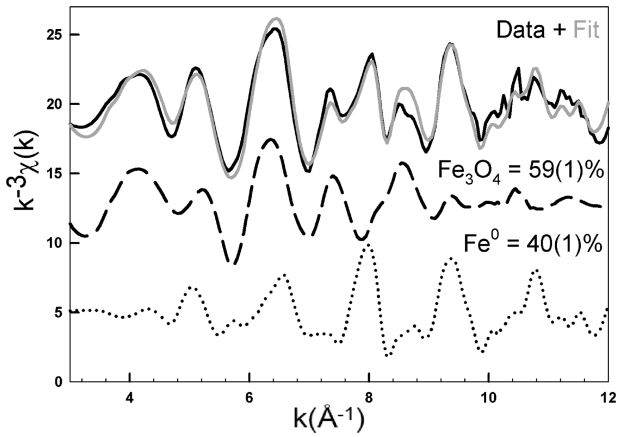

FIGURE 4. LCF of the EXAFS spectrum of NZVI aged for 1 month in deoxygenated water with corresponding speciation data and uncertainty for the last digit in parentheses. The solid black line = data, the solid gray line = fit, the dashed black line = magnetite, and the dotted black line = Fe^0 foil. From the unaged NZVI, shown in Figure 3, the sulfate species has disappeared and magnetite layer has spread; consequently, the amount of Fe^0 has dropped by 20%.

In the presence of dissolved oxygen, it is plausible that the formation of Fe^{3+}-only species, instead of mixed Fe^{2+}/Fe^{3+} species, could occur at the surface of the NZVI particle. Due to the limited extent of the oxide layer in NZVI and the similar spinel crystal structure of both maghemite and magnetite, their differentiation by XRD is very difficult (*38*). EXAFS analysis using high quality, well-characterized model compound spectra is more sensitive to interatomic distances and coordination number rather than lattice spacing and is capable of providing quantitative information regarding the amounts of each constituent in a sample. The distinction between these two phases and quantifying them is an important objective of the field of nanoparticle engineering; because it is the surfaces of such particles and the associated physicochemical properties (e.g., surface charge) that govern the biotic and abiotic interactions these particles will face in the environment including, e.g., deposition, attachment to bacteria, and aggregation.

LCF of the initial starting material (Figure 3), a dry powder, showed that Fe^0, magnetite, and an iron-sulfate species, e.g., schwertmannite, were the dominant mineral phases present. This finding is different from previously published papers that have characterized the precursor material in its aqueous slurry phase (RNIP 10-DS). These studies have the composition of slurry particles to be between 30 and 70% Fe^0 content (*17, 20*), and commonly, the balance is assumed to be magnetite. The presence of schwertmannite in the dry powder starting material is likely due to the high initial amounts of sulfur in the particles of 0.5 wt % (*20*) and the precipitation of schwertmannite upon drying to form the dry powder (RNIP 10-DP). EXAFS LCF of the dry starting material that was aged for 1 month in deoxygenated water in an anaerobic glovebox agreed with previous results with the bulk particles containing 40% ± 1% Fe^0 and 59% ± 1% Fe_3O_4 (Figure 4). Brief exposure to water alone or in the presence of any anion causes disappearance of schwertmannite and oxidation of Fe^0 to magnetite; as all of the 1 month aged samples have similar composition to Figure 4. After 6 months of exposure in anaerobic water, the composition changed to 38.4% ± 0.6% Fe^0 and 70% ± 2% magnetite due to continuing oxidation of Fe^0 by water-derived protons (Figure 3).

The passivation effect of nitrate is further reinforced by comparing the results of EXAFS analysis of the unreacted NZVI particles (10-DP unexposed to water) and NZVI particles after 6 months of aging in 10 mN nitrate (Figure 3). The unreacted NZVI and the 6 month aged sample in 10 mN nitrate both contain Fe^0, schwertmannite, and magnetite in similar proportions. This effect is unique among the reactions that occurred in the presence of anions because not only did the nitrate passivate the surface from further oxidation but also passivation occurred rapidly enough to limit schwertmannite disappearance and formation of any additional mineral phases.

NZVI aged in the presence of phosphate or sulfate for 1 month had only Fe^0 and Fe_3O_4 (Supporting Information, Figures S2 and S3). NZVI particles aged for ≥6 months in the presence of phosphate or sulfate formed vivianite, $Fe_3(PO_4)_2 \cdot 8H_2O$ (Figure 3) or Fe−S minerals, e.g., schwertmannite, $Fe^{3+}16O_{16}(OH,SO_4)_{12-13} \cdot 10-12H_2O$ (Figure 3), respectively. There was also a significant decrease in the amount of Fe^0 in both batches of 6 month aged particles to ∼9%. A previous column study involving Fe^0 and contaminated groundwater also reported the formation of iron−sulfur mineral phases

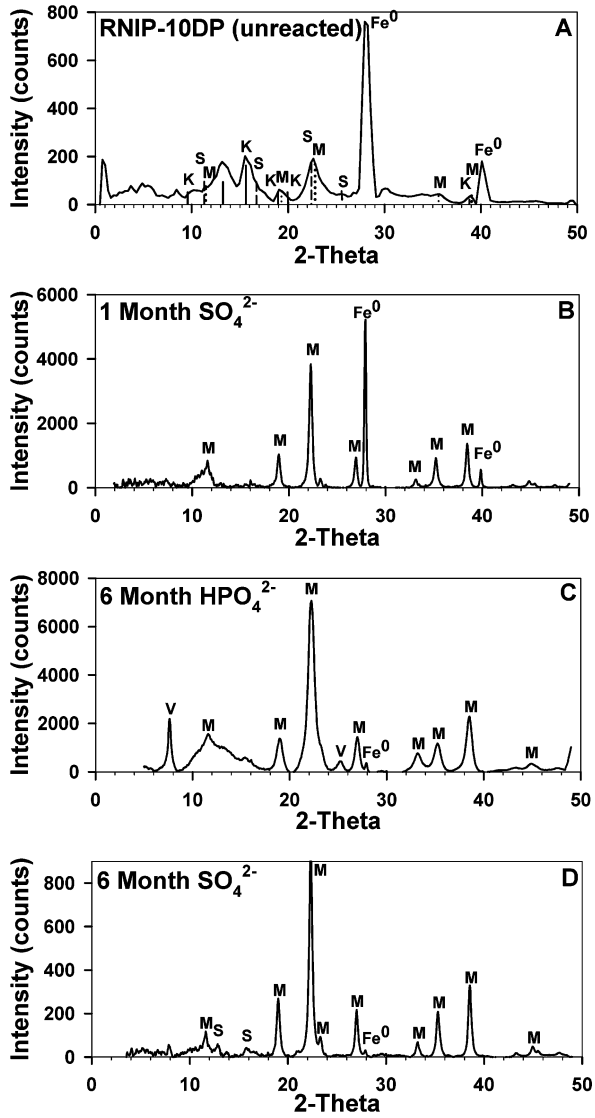

FIGURE 5. (A–D). XRD patterns of unreacted and exposed NZVI, in 10 mN sulfate and phosphate. (A) = dry-unreacted RNIP showing the presence of mostly Fe^0, with some magnetite and iron sulfate species (schwertmannite and mikasaite). (B) = NZVI aged for 1 month in sulfate, where the sulfate species from (A) have disappeared and magnetite has increased in proportion to Fe^0. (C) = 6 month aged in phosphate; vivianite peaks appear at ~7° and 25° 2θ. (D) = 6 month aged in sulfate; indications of schwertmannite arise as peaks at ~13° and 16° 2θ. Species symbols and line styles in (A) indicated in parentheses: Fe^0 is labeled as such, M = magnetite (dotted), S = schwertmannite (dashed), K = mikasaite/$Fe_2(SO_4)_3$ (solid line). Vivianite only appears in (C) and is represented by V. (A) has been cropped to show more detail below 800 counts. The peak at ~28° 2θ has a maximum value of ~1000 counts.

and other precipitates (*39*). The presence of mineral phases in addition to Fe^0 and Fe_3O_4 typically reported suggests that these phases could affect NZVI behavior in aqueous environments containing common solutes such as sulfate (e.g., in marine environments).

XRD analysis of the powdered starting material and the sulfate and phosphate aged samples is consistent with the EXAFS results. The unreacted RNIP 10-DP (Figure 5a) is dominated by peaks for Fe^0 but contains less-intense peaks for magnetite and schwertmannite. The peaks from 15°–25° 2θ, of Figure 5a, match several iron sulfate XRD cards to differing degrees. The two species that matched the closest were schwertmannite and mikasaite, $Fe_2(SO_4)_3$, but it could neither be determined which was more likely nor confirmed using EXAFS because a model compound of mikasaite was not available. After 1 month of aging in the presence of sulfate (Figure 5b) or phosphate (not shown, but identical to sulfate), the particles are predominately Fe^0 and Fe_3O_4. However, after 6 months of aging, vivianite peaks (7.5° 2θ and several) appear in the XRD pattern for the phosphate aged sample (Figure 5c) and an iron sulfate species appears in the sulfate aged sample (Figure 5d), matching schwertmannite.

Effect of Dissolved Oxygen (DO). After 24 h of exposure to O_2-saturated ($pO_2 = 0.21$ atm) water, some NZVI had visibly turned from black to dark brown/orange, suggesting the formation of an iron oxide phase other than magnetite, which is black. EXAFS LCF analysis of these particles indicated growth of maghemite within the oxide layer and near complete oxidation of Fe^0 in the particles. The composition of the DO exposed particles was 2.1% ± 0.5% Fe^0, 77.7% ± 9.5% Fe_3O_4, and 15.4% ± 10.3% γ-Fe_2O_3 (Supporting Information, Figure S4). Maghemite was not observed in any of the 6 month aged particles in anaerobic solutions. The growth of maghemite is likely due to oxidation of the magnetite layer which occurs once the Fe^0 in the particle core is oxidized. Previous results have shown that maghemite can be synthesized from magnetite (*14*). Besides the increased amount of oxidation, the dramatic increase in rate of Fe^0 oxidation, in the presence of dissolved oxygen compared to samples aged anaerobically for 1 and 6 months, has critical implications toward NZVI speciation and reactivity, especially the reducing power and reactive lifetime when used as a remediation agent.

Implications for the Application of NZVI and for the Environment. There are several implications of this study regarding the effectiveness and safety surrounding the use of NZVI for groundwater remediation. First, the presence of common groundwater anions does not appear to inhibit the oxidation of NZVI in the long term. This implies that complete oxidation of the Fe^0 in the particles under in situ conditions is possible. One exception is nitrate which passivates the surface, thereby encapsulating the Fe^0 and decreasing particle reactivity. The effect of this passivation on NZVI toxicity has not been studied. This precludes NZVI use in areas with high concentrations of nitrate as a cocontaminant (e.g., Oak Ridge National Laboratory (*40*)). The formation of additional mineral phases (e.g., vivianite- and schwertmannite-like phases) on the particle surfaces other than the typically reported magnetite may affect the reactivity of the NZVI with contaminants as well as the interaction potential between NZVI and aquifer media and biological receptors, thereby affecting exposure and toxicity potential.

Dissolved oxygen very rapidly oxidizes NZVI and can cause the formation of maghemite along with magnetite. Any DO in groundwater will, therefore, use Fe^0 that would otherwise have been used for contaminant degradation, thereby requiring more NZVI to treat a given mass of contaminant than when applied under anaerobic conditions. The loss of Fe^0 from NZVI and an increase in the maghemite to magnetite ratio in NZVI exposed to DO can decrease aggregation and increase transport in porous media (*9*) and, therefore, increase potential for exposure. Conversely, the potential biological effects of NZVI to subsurface microorganisms and to human health will decrease with increasing oxidation to Fe^{3+} oxides such as maghemite (*11, 12*). The effect of common groundwater constituents on the overall fate, transport, reactivity, and potential toxicity of NZVI discussed here suggest that an understanding of the site geochemistry is needed to evaluate potential effectiveness and safety of NZVI as a remediation strategy.

Acknowledgments

This material is based upon work supported by the National Science Foundation (NSF) and the Environmental Protection Agency (EPA) under NSF Cooperative Agreement EF-0830093, Center for the Environmental Implications of Nanotechnology (CEINT), NSF (BES-0608646), and EPA (R833326). Any opinions, findings, conclusions or recommendations expressed in this material are those of the author(s) and do not necessarily reflect the views of the NSF or the EPA. This work has not been subjected to EPA review, and no official endorsement should be inferred. Portions of this research were carried out at the Stanford Synchrotron Radiation Laboratory, a national user facility operated by Stanford University on behalf of the U.S. Department of Energy, Office of Basic Energy Sciences. We thank James Dale, John Stegemeier, and members of the Environmental Geochemistry Lab at Chapman University for sample preparation and analysis support, as well as the staff and beamline scientists at SSRL.

Supporting Information Available

The model compounds synthesis procedures, EXAFS of model compounds, individual EXAFS and respective LCF results of NZVI aged for 1 month in different anionic solutions, and the EXAFS and LCF results of NZVI exposed to excess DO. This material is available free of charge via the Internet at http://pubs.acs.org.

Literature Cited

(1) Zhang, W. X. Nanoscale iron particles for environmental remediation: An overview. *J. Nanopart. Res.* **2003**, *5* (3−4), 323–332.

(2) Kanel, S. R.; Goswami, R. R.; Clement, T. P.; Barnett, M. O.; Zhao, D. Two dimensional transport characteristics of surface stabilized zero-valent iron nanoparticles in porous media. *Environ. Sci. Technol.* **2008**, *42* (3), 896–900.

(3) Saleh, N.; Kim, H. J.; Phenrat, T.; Matyjaszewski, K.; Tilton, R. D.; Lowry, G. V. Ionic strength and composition affect the mobility of surface-modified Fe-0 nanoparticles in water-saturated sand columns. *Environ. Sci. Technol.* **2008**, *42* (9), 3349–3355.

(4) Saleh, N.; Phenrat, T.; Sirk, K.; Dufour, B.; Ok, J.; Sarbu, T.; Matyjaszewski, K.; Tilton, R. D.; Lowry, G. V. Adsorbed triblock copolymers deliver reactive iron nanoparticles to the oil/water interface. *Nano Lett.* **2005**, *5* (12), 2489–2494.

(5) Sirk, K. M.; Saleh, N. B.; Phenrat, T.; Kim, H. J.; Dufour, B.; Ok, J.; Golas, P. L.; Matyjaszewski, K.; Lowry, G. V.; Tilton, R. D. Effect of Adsorbed Polyelectrolytes on Nanoscale Zero Valent Iron Particle Attachment to Soil Surface Models. *Environ. Sci. Technol.* **2009**, *43* (10), 3803–3808.

(6) Puls, R. W.; Blowes, D. W.; Gillham, R. W. Long-term performance monitoring for a permeable reactive barrier at the US Coast Guard Support Center, Elizabeth City, North Carolina. *J. Hazard. Mater.* **1999**, *68* (1−2), 109–124.

(7) Phillips, D. H.; Watson, D. B.; Roh, Y.; Gu, B. Mineralogical characteristics and transformations during long-term operation of a zerovalent iron reactive barrier. *J. Environ. Qual.* **2003**, *32* (6), 2033–2045.

(8) Lemos, V. P.; da Costa, M. L.; Lemos, R. L.; de Faria, M. S. G. Vivianite and siderite in lateritic iron crust: An example of bioreduction. *Quim. Nova* **2007**, *30* (1), 36–40.

(9) Phenrat, T.; Saleh, N.; Sirk, K.; Tilton, R. D.; Lowry, G. V. Aggregation and sedimentation of aqueous nanoscale zerovalent iron dispersions. *Environ. Sci. Technol.* **2007**, *41* (1), 284–290.

(10) Liu, Y. Q.; Lowry, G. V. Effect of particle age (Fe-o content) and solution pH on NZVI reactivity: H-2 evolution and TCE dechlorination. *Environ. Sci. Technol.* **2006**, *40* (19), 6085–6090.

(11) Phenrat, T.; Long, T. C.; Lowry, G. V.; Veronesi, B. Partial oxidation ("aging") and surface modification decrease the toxicity of nanosized zerovalent iron. *Environ. Sci. Technol.* **2009**, *43* (1), 195–200.

(12) Auffan, M.; Achouak, W.; Rose, J.; Roncato, M. A.; Chaneac, C.; Waite, D. T.; Masion, A.; Woicik, J. C.; Wiesner, M. R.; Bottero, J. Y. Relation between the redox state of iron-based nanoparticles and their cytotoxicity toward Escherichia coli. *Environ. Sci. Technol.* **2008**, *42* (17), 6730–6735.

(13) Wiesner, M. R.; Lowry, G. V.; Alvarez, P.; Dionysiou, D.; Biswas, P. Assessing the risks of manufactured nanomaterials. *Environ. Sci. Technol.* **2006**, *40* (14), 4336–4345.

(14) Cornell, R. M.; Schwertmann, U., *The Iron Oxides: Structure, Properties, Reactions, Occurrences and Uses*, 2 ed.; Wiley-VCH: Weinheim, Germany, 2003; pp 129, 235, 506−508, 537−538, 506−508.

(15) Phenrat, T.; Kim, H. J.; Fagerlund, F.; Illangasekare, T.; Tilton, R. D.; Lowry, G. V. Particle size distribution, concentration, and magnetic attraction affects transport of polymer-modified Fe^0 nanoparticles in sand columns. *Environ. Sci. Technol.* **2009**, *43* (13), 5079–5085.

(16) Sarathy, V.; Tratnyek, P. G.; Nurmi, J. T.; Baer, D. R.; Amonette, J. E.; Chun, C. L.; Penn, R. L.; Reardon, E. J. Aging of iron nanoparticles in aqueous solution: Effects on structure and reactivity. *J. Phys. Chem. C* **2008**, *112* (7), 2286–2293.

(17) Nurmi, J. T.; Tratnyek, P. G.; Sarathy, V.; Baer, D. R.; Amonette, J. E.; Pecher, K.; Wang, C. M.; Linehan, J. C.; Matson, D. W.; Penn, R. L.; Driessen, M. D. Characterization and properties of metallic iron nanoparticles: Spectroscopy, electrochemistry, and kinetics. *Environ. Sci. Technol.* **2005**, *39* (5), 1221–1230.

(18) Van Der Zee, C.; Slomp, C. P.; Rancourt, D. G.; De Lange, G. J.; Van Raaphorst, W. A Mossbauer spectroscopic study of the iron redox transition in eastern Mediterranean sediments. *Geochim. Cosmochim. Acta* **2005**, *69* (2), 441–453.

(19) Liu, Y. Q.; Choi, H.; Dionysiou, D.; Lowry, G. V. Trichloroethene hydrodechlorination in water by highly disordered monometallic nanoiron. *Chem. Mater.* **2005**, *17* (21), 5315–5322.

(20) Liu, Y. Q.; Majetich, S. A.; Tilton, R. D.; Sholl, D. S.; Lowry, G. V. TCE dechlorination rates, pathways, and efficiency of nanoscale iron particles with different properties. *Environ. Sci. Technol.* **2005**, *39* (5), 1338–1345.

(21) Baer, D. R.; Amonette, J. E.; Engelhard, M. H.; Gaspar, D. J.; Karakoti, A. S.; Kuchibhatla, S.; Nachimuthu, P.; Nurmi, J. T.; Qiang, Y.; Sarathy, V.; Seal, S.; Sharma, A.; Tratnyek, P. G.; Wang, C. M. Characterization challenges for nanomaterials. *Surf. Interface Anal.* **2008**, *40* (3−4), 529–537.

(22) Wang, C. M.; Baer, D. R.; Thomas, L. E.; Amonette, J. E.; Antony, J.; Qiang, Y.; Duscher, G. Void formation during early stages of passivation: Initial oxidation of iron nanoparticles at room temperature. *J. Appl. Phys.* **2005**, *98* (9), XXXX.

(23) O'Day, P. A.; Rivera, N.; Root, R.; Carroll, S. A. X-ray absorption spectroscopic study of Fe reference compounds for the analysis of natural sediments. *Am. Mineral.* **2004**, *89* (4), 572–585.

(24) Waychunas, G. A.; Apted, M. J.; Brown, G. E. X-Ray K-edge absorption-spectra of Fe minerals and model compounds - near-edge structure. *Phys. Chem. Miner.* **1983**, *10* (1), 1–9.

(25) Brown, G. E.; Calas, G.; Waychunas, G. A.; Petiau, J. X-ray absorption spectroscopy and its applications in mineralogy and geochemistry. *Rev. Mineral.* **1988**, *18*, 431–512.

(26) Waychunas, G. A.; Brown, G. E.; Apted, M. J. X-Ray K-Edge absorption-spectra of Fe minerals and model compounds 2. EXAFS. *Phys. Chem. Miner.* **1986**, *13* (1), 31–47.

(27) Liu, Y.; Phenrat, T.; Lowry, G. V. Effect of TCE concentration and dissolved groundwater solutes on NUI-Promoted TCE dechlorination and H_2 evolution. *Environ. Sci. Technol.* **2007**, *41* (22), 7881–7887.

(28) Webb, S. M. SIXpack: a graphical user interface for XAS analysis using IFEFFIT. *Phys. Scr.* **2005**, *T115*, 1011–1014.

(29) Ressler, T.; Wong, J.; Roos, J.; Smith, I. L. Quantitative speciation of Mn-bearing particulates emitted from autos burning (methylcyclopentadienyl)manganese tricarbonyl-added gasolines using XANES spectroscopy. *Environ. Sci. Technol.* **2000**, *34* (6), 950–958.

(30) Ostergren, J. D.; Brown, G. E., Jr.; Parks, G. A.; Tingle, T. N. Quantitative speciation of lead in selected mine tailings from Leadville, CO. *Environ. Sci. Technol.* **1999**, *33* (10), 1627–1636.

(31) Kim, C. S.; Brown, G. E.; Rytuba, J. J. Characterization and speciation of mercury-bearing mine wastes using X-ray absorption spectroscopy. *Sci. Total Environ.* **2000**, *261* (1−3), 157–168.

(32) Lande, J., Webb, S. *The Area Diffraction Machine*, 1.0; 2007.

(33) Hem, J. D. *Study and interpretation of the chemical characteristics of natural water*, 3rd ed.; U.S. Geological Survey Water Supply Paper 2254, 1985; pp 109−130.

(34) Harter, T. Groundwater quality and groundwater pollution, FWQP Reference Sheet 11.2, in UC Davis ANR Publication 8084. http://groundwater.ucdavis.edu/Publications/Harter_FWQFS_8084.pdf.

(35) Schlicker, O.; Ebert, M.; Fruth, M.; Weidner, M.; Wust, W.; Dahmke, A. Degradation of TCE with iron: The role of competing chromate and nitrate reduction. *Ground Water* **2000**, *38* (3), 403–409.

(36) Mishra, D.; Farrell, J. Understanding nitrate reactions with zerovalent iron using tafel analysis and electrochemical impedance spectroscopy. *Environ. Sci. Technol.* **2005**, *39* (2), 645–650.
(37) Kohn, T.; Livi, K. J. T.; Roberts, A. L.; Vikesland, P. J. Longevity of granular iron in groundwater treatment processes: Corrosion product development. *Environ. Sci. Technol.* **2005**, *39* (8), 2867–2879.
(38) Signorini, L.; Pasquini, L.; Savini, L.; Carboni, R.; Boscherini, F.; Bonetti, E.; Giglia, A.; Pedio, M.; Mahne, N.; Nannarone, S. Size-dependent oxidation in iron/iron oxide core-shell nanoparticles. *Phys. Rev. B* **2003**, *68* (19), XXXX.
(39) Kober, R.; Schlicker, O.; Ebert, M.; Dahmke, A. Degradation of chlorinated ethylenes by Fe-0: inhibition processes and mineral precipitation. *Environ. Geol.* **2002**, *41* (6), 644–652.
(40) Wu, W. M.; Carley, J.; Fienen, M.; Mehlhorn, T.; Lowe, K.; Nyman, J.; Luo, J.; Gentile, M. E.; Rajan, R.; Wagner, D.; Hickey, R. F.; Gu, B. H.; Watson, D.; Cirpka, O. A.; Kitanidis, P. K.; Jardine, P. M.; Criddle, C. S. Pilot-scale in situ bioremediation of uranium in a highly contaminated aquifer. 1. Conditioning of a treatment zone. *Environ. Sci. Technol.* **2006**, *40* (12), 3978–3985.

ES902924H

Chemical transformations during aging of zero-valent iron nanoparticles in the presence of common groundwater dissolved constituents

Supporting Information

Brian C. Reinsch[1,2], Brady Forsberg[3], R. Lee Penn[3], Christopher S. Kim[4], Gregory V. Lowry[1,2]*

glowry@andrew.cmu.edu

telephone: 412-268-2948

fax: 412-268-7813

*Carnegie Mellon University

Dept. Civil & Environmental Engineering

5000 Forbes Ave.

Pittsburgh, PA 15213-3890

[1] Department of Civil and Environmental Engineering, Carnegie Mellon University, Pittsburgh, PA 152313.

[2] Center for the Environmental Implications of Nanotechnology (CEINT), Pittsburgh, PA 15213.

[3] Department of Chemistry, University of Minnesota, Minneapolis, MN 55455

[4] Department of Chemistry, Chapman University, Orange, CA 92866

Supporting Information (SI)

The supporting information consists of 7 additional pages number S1 – S10 and contains information regarding the synthesis of model compounds used for the extended X-ray absorption fine structure (EXAFS) linear combination fitting (LCF) of samples discussed in the manuscript and a detailed description of the X-ray absorption spectroscopy (XAS) data collection and analysis methods. In addition, there are six figures labeled Figure S1 – S4 and a list of the literature cited within SI. Figure S1 shows the compiled background subtracted Fe K-edge EXAFS for the model compounds used in this study. Figures S2 – S4 are the resulting spectra and LCF fitting of NZVI selected samples aged for 1 month.

Model Compound Synthesis:

All solutions unless otherwise stated were carried out in deionized Milli-Q water (18Ω), and all chemicals were of reagent grade quality.

6-Line Ferrihydrite: 6 nm dots - The synthesis method was adapted from Cornell and Schwertmann (*1*). While stirring, 20g of solid $Fe(NO_3)_3 \cdot 9H_2O$ was added to 2.0 L of Milli-Q H_2O at 75°C. The solution temperature was maintained at 75°C for 12 min. After heating, the solution was plunged into an ice bath until it reached ~20°C (~30 min). The cooled suspension was placed into dialysis bags versus Milli-Q H_2O. The water was changed three times per day for three days. The resulting suspension was placed in a number of weigh boats, covered, and placed in a fume hood to dry. Using a mortar and pestle, the dry, dark reddish brown particles were ground into a fine powder and stored in a glass vial.

Goethite: The synthesis of the nanorods began by using the 6-Line Ferrihydrite synthesis procedure adapted from (*2*). Post-dialysis, the pH of the ferrihydrite suspension was quickly converted to 12 using 5 M NaOH (Fisher, ACS grade). A deep maroon suspension formed. The suspension was heated at 90°C for 24 h, after which a deep orange precipitate was present. The suspension was placed into dialysis bags versus Milli-Q H_2O after removing the supernatant solution. The water was changed three times per day for three days. The resulting suspension was placed in a number of weigh boats, covered, and placed in a fume hood to dry. Using a

mortar and pestle, the dry, orange particles were ground into a fine powder and stored in a glass vial.

Green Rust: Synthesis adapted from Schwertmann, and Fechter (*3*). Green Rust was prepared by titrating $FeSO_4$ (0.1 M, 250mL) with NaOH (0.1 M) until the pH reached 6.5-7 under constant N_2 bubbling at room temperature. The solution was then slowly oxidized with a bubbling of air until while maintaining the pH of the solution at 6.5-7 with additional NaOH if needed. Upon partial oxidation a green-gray precipitate formed, and the system was moved to a N_2-H_2 chamber to avoid further oxidation. This precipitate was filtered and allowed to dry in the N_2-H_2 chamber by placing it within covered weigh boats.

Lepidocrocite: Synthesis adapted from Ona-Nguema, et al. 2002 (*4*). Synthetic lepidocrocite was obtained by mixing $FeCl_2 \cdot 4H_2O$(0.228 M) with NaOH (0.4 M) until the pH of the solution reached 7, and precipitation occurred. The suspension was magnetically stirred under constant aeration to ensure oxidation of the solid. The suspension was stirred for 3 hours, at room temperature, and the resulting solid was washed multiple times with Milli-Q water to remove electrolytes. The lepidocrocite was then placed within weight boats, covered, and was allowed to dry in the fume hood.

Pyrite: Synthesis adapted from Kar and Chaudhuri, 2004 (*5*). Synthetic pyrite was obtained by placing $Fe(NO_3)_3 \cdot 9H_2O$ and thiourea (NH_2CSNH_2) in a 1:4 molar ratio within a Teflon lined hydrothermal bomb chamber (110 mL capacity). The chamber was filled to approximately 80% volume with ethylenediamine ($NH_2CH_2CH_2NH_2$) and then stirred for 30 min at room temperature. The chamber was sealed and placed within the hydrothermal bomb and then placed within a box furnace at 180 °C for 12 h. The resulting black precipitate was filtered and washed several times in ethanol to remove any salts or other impurities. The Precipitate was then dried at 120 °C for 6 h to obtain a black powder.

Siderite: Synthesis adapted from Rakshit et al. (*6*). Synthetic siderite was prepared using Milli-Q water that was made anoxic by purging for three hours with N_2. The reaction was carried out in

an N_2-H_2 chamber to ensure a completely anoxic environment. To a $FeCl_2$ solution (0.5 M), equimolar amounts of Na_2CO_3 were slowly added with stirring at room temperature. This resulted in a pale gray precipitate which was washed with anoxic Milli-Q water to remove electrolytes. The siderite solid was stored in suspension until needed, and was dried within the N_2-H_2 chamber by placing within covered weigh boats.

Schwertmannite: Synthesis method from Cornell and Schwertmann (*7*). The reaction was carried out using 2 L of Milli-Q water. The water was heated to 75 ºC and then 10.8 g $FeCl_3$ and Na_2SO_4 while stirring. The solution was dialyzed for two days. The solid was isolated by centrifugation, and the resulting solid was washed several times with ethanol and the precipitate was dried in an anaerobic glovebox by evaporation.

Vivianite: Synthesis adapted from Eynard et al. 1992 (*8*). Synthetic vivianite was obtained through the slow neutralization of $FeSO_4$ (0.05 M) in H_3PO_4 (0.035 M, 250 mL) with KOH (0.05 M) at room temperature. The pH of the mixture was brought up to 6, where the precipitation of a blue-grey powder occurred. The powder was washed via centrifugation with Milli-Q water to remove the presence of salts, placed in a number of weigh boats, covered, and placed within the fume hood to dry. Using a mortar and pestle, the blue-gray powder solid was ground into a powder and stored in a glass vial.

X-ray absorption spectroscopy (XAS) analysis:

X-ray absorption spectroscopy (XAS) was conducted at Stanford Synchrotron Radiation Laboratory (SSRL) wiggler magnet beamline 10-2 under anaerobic conditions. A 1:10 mass dilution of dry powder sample to boron nitride powder was conducted to optimize the amount of beam that was absorbed by the sample. The resulting dilution was placed into 1.5 mm thick Teflon holders and sealed with Kapton tape. Loaded samples were transported from the glovebox to the experimental station, or hutch, inside an airtight box, removed and loaded into a sample chamber. N_2 was flowed through the sample chamber during analysis in order to keep the sample in an anaerobic environment to prevent iron oxidation in air. X-ray absorption spectroscopy was performed using a double Si 111 monochromator crystal with the beam detuned 30% from

maximum intensity to reduce harmonic signals. Fe K-edge (7112 eV) XAS spectra were collected at room temperature in transmission mode using a Fe calibration foil over the energy range 6879-7986 eV.

Data were analyzed using SixPACK software version 0.60 (*9*). XAS scans were calibrated for changes in assigned monochromator energy to 7112.0 eV by using the first derivative of the Fe calibration standard and averaged together. These spectra were deglitched when needed. Background subtraction was performed using SixPACK with E_0 defined as 7125 eV, and R-background = 1.0 Å. The resulting spectra were converted to frequency (k) space, weighted by k^3.

The principal component analyses (PCA) were also performed in SixPACK, which uses an algorithm described by Ressler et al. (*10*) and references therein, to determine the minimum number of components that could be used to model the sample set of 1 month and 6 month aged EXAFS spectra, respectively, and account for >90% of the spectra; a value chosen because the addition of another component would not significantly raise the cumulative variance with respect to 100% and would not likely improve the fit of the model significantly during LCF. EXAFS spectra of a series of related compounds can be statistically analyzed using (PCA), which yields information regarding the number of components/unique species that can be used to describe, or fit, the data within experimental error (*11*). PCA was conducted in k-space in the k-range of 3-12, 3-15 or 3-17, depending on the quality of the EXAFS data. The number of allowable components was always ≤3; as determined to represent >90% of the sample spectra. The results from PCA were applied to LCF to provide quantitative speciation information.

In order to successfully identify all mineral phases present in batch studies a model compound database of nano-sized Fe mineral extended X-ray absorption fine structure (EXAFS) spectra was compiled. The model compound library consisted of common Fe-oxides, Fe-hydroxides, and Fe mineral phases that possibly could have formed from the reaction of groundwater anions (e.g. magnetite, maghemite, pyrite, schwertmannite, vivianite, goethite). A complete list of the model compounds along with their EXAFS spectra and other measured properties are provided (Figure S1). Samples of model compounds were dried anaerobically into powders and diluted into boron nitride powder prior to X-ray analysis. EXAFS spectra were collected using the same SSRL beamline and parameters described above.

LCF of individual sample EXAFS spectra with a well defined and comprehensive model compound library were used to identify the mineral phases present in a sample and to quantify the amount of each phase that is present in the bulk sample, with the number of phases allowed to exist constrained to the number of components that was determined by PCA. The validity of the linear combination fits is related to how comprehensive the model compound library is that is used to fit the data and the quality of the individual spectra. Additionally, identified components should be considered accurate to ±25% of their stated values while components representing less than 10% of a fit should be viewed with caution (*12, 13*).The linear least squares fitting procedure employed was adapted from Kim et al. (*13*). The spectra were fit from a k-range of 3-15 or 3-17, depending on the quality of the EXAFS data, and at no time were the fits scaled or forced to total 100%, so that the accuracy of model compound fits could be transparent. However, by limiting the number of components by using PCA and the methodical LCF procedure from Kim et. al. (*13*) to only the significant contributors there may be some fits that do not total 100%.

Figures:

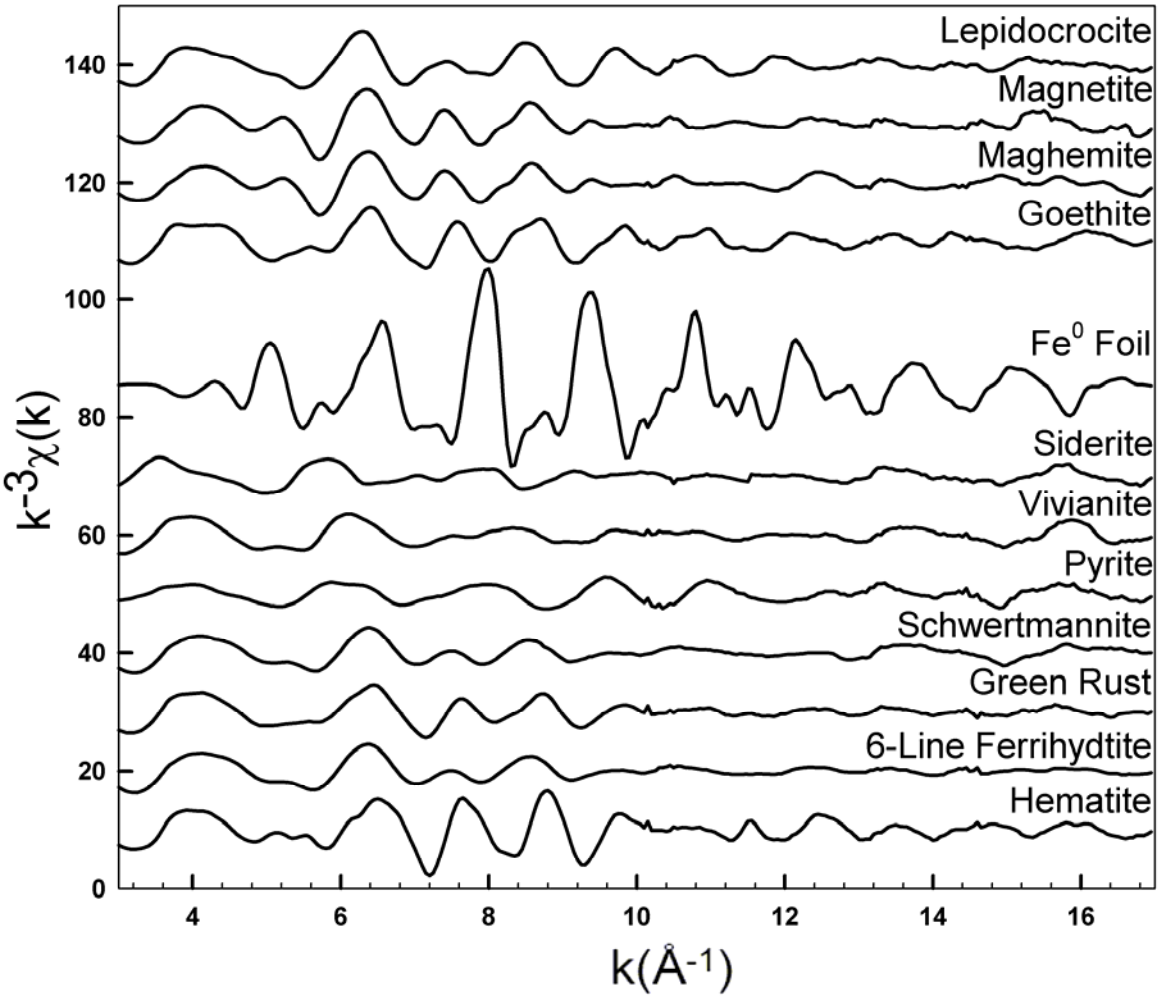

Figure S1. EXAFS spectra of Fe mineral model compounds used for LCF of heterogeneous NZVI Samples. The horizontal axis represents the conversion of energy to momentum space following the normalization of the EXAFS data to a fixed point in energy space. The vertical axis is a k^3-weighted expression of the EXAFS function.

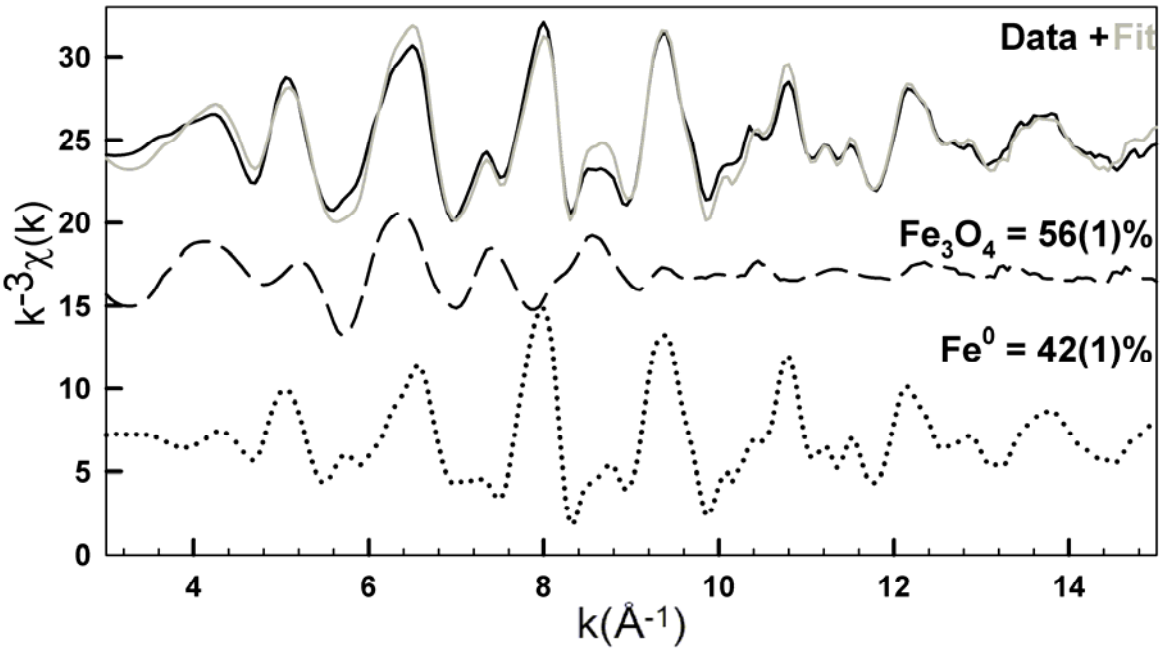

Figure S2. EXAFS data and LCF of NZVI aged anaerobically for 1 month in 10 mN HPO_4^{2-} solution with the corresponding speciation data and uncertainty for the last digit in parenthesis. The black line = data, grey line = fit, the dashed line = magnetite, and the dotted line = Fe^0. From the original composition of the starting material these particles have lost their iron-sulfate character and oxidized from ~60% Fe^0 to 60% magnetite.

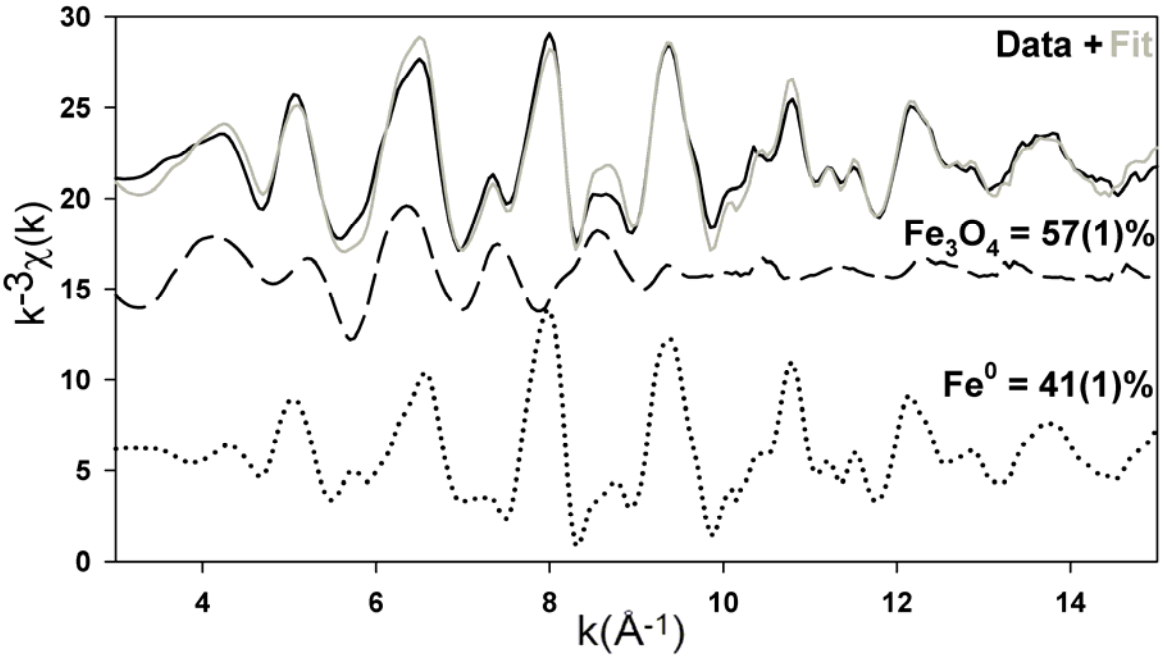

Figure S3. EXAFS LCF results for NZVI aged anaerobically for 1 month in 10 mN SO_4^{2-} solution with the speciation data and related uncertainty for the last digit shown in parenthesis. The black line = data, grey line = fit, dashed line = magnetite, and dotted line = Fe^0. Simmilar to the other anions after 1 month, the particles have lost the iron-sulfate species that was prevalent in the starting material and magnetite has become the dominant phase of oxidized iron.

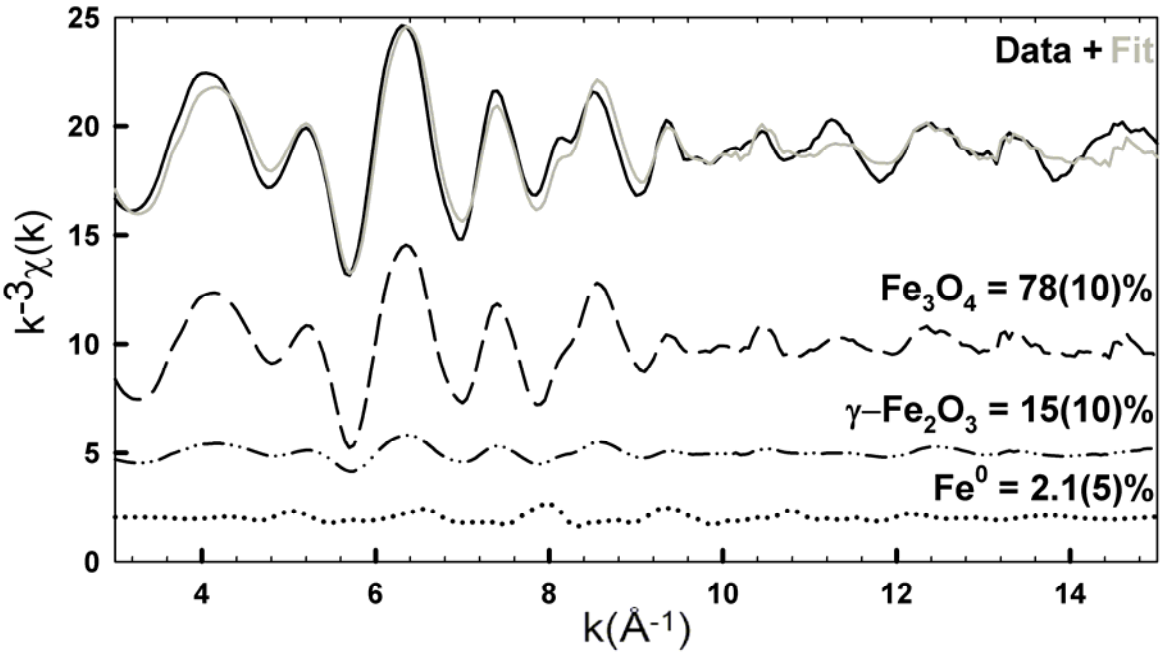

Figure S4. EXAFS data and LCF results of NZVI exposed to excess DO for 24 hours with respective uncertainties of the last digit in parenthesis. The black line = data, grey line = fit, dashed line = magnetite, dash-dot-dot line = maghemite, and dotted line = Fe^0. After only 24 hours Fe^0 is almost completely depleted and maghemite forms.

References:

(1) Cornell, R. M.; Schwertmann, U., *The Iron Oxides: Structure, Properties, Reactions, Occurrences and Uses*, 2 ed.; Wiley-VCH: Weinheim, Germany, 2003; p 533.

(2) Burleson, D. J.; Penn, R. L. Two-step growth of goethite from ferrihydrite. *Langmuir* **2006,** *22* (1), 402-409.

(3) Schwertmann, U.; Fechter, H. The formation of green rust and its transformation to lepidocrocite. *Clay Minerals* **1994,** *29* (1), 87-92.

(4) Ona-Nguema, G.; Abdelmoula, M.; Jorand, F.; Benali, O.; Gehin, A.; Block, J. C.; Genin, J. M. R. Iron(II,III) hydroxycarbonate green rust formation and stabilization from lepidocrocite bioreduction. *Environ. Sci. Technol.* **2002,** *36* (1), 16-20.

(5) Kar, S.; Chaudhuri, S. Solvothermal synthesis of nanocrystalline FeS_2 with different morphologies. *Chemical Physics Letters* **2004,** *398* (1-3), 22-26.

(6) Rakshit, S.; Matocha, C. J.; Coyne, M. S. Nitrite reduction by siderite. *Soil Science Society of America Journal* **2008,** *72* (4), 1070-1077.

(7) Cornell, R. M.; Schwertmann, U., *The Iron Oxides: Structure, Properties, Reactions, Occurrences and Uses*, 2 ed.; Wiley-VCH: Weinheim, Germany, 2003; pp 129, 235, 506-508, 537-538, 506-508.

(8) Eynard, A.; Delcampillo, M. C.; Barron, V.; Torrent, J. Use of vivianite ($Fe_3(PO_4)_{2.8}H_2O$) to prevent iron chlorosis in calcareous soils. *Fertilizer Research* **1992,** *31* (1), 61-67.

(9) Webb, S. M. SIXpack: a graphical user interface for XAS analysis using IFEFFIT. *Phys. Scr.* **2005,** *T115*, 1011-1014.

(10) Ressler, T.; Wong, J.; Roos, J.; Smith, I. L. Quantitative speciation of Mn-bearing particulates emitted from autos burning (methylcyclopentadienyl)manganese tricarbonyl-added gasolines using XANES spectroscopy. *Environ. Sci. Technol.* **2000,** *34* (6), 950-958.

(11) Wasserman, S. R.; Allen, P. G.; Shuh, D. K.; Bucher, J. J.; Edelstein, N. M. EXAFS and principal component analysis: a new shell game. *J. Synchrotron Radiat.* **1999,** *6*, 284-286.

(12) Ostergren, J. D.; Brown, G. E., Jr.; Parks, G. A.; Tingle, T. N. Quantitative speciation of lead in selected mine tailings from Leadville, CO. *Environ. Sci. Technol.* **1999,** *33* (10), 1627-1636.

(13) Kim, C. S.; Brown, G. E.; Rytuba, J. J. Characterization and speciation of mercury-bearing mine wastes using X-ray absorption spectroscopy. *Sci. Total Environ.* **2000,** *261* (1-3), 157-168.